Nanotechnology, Nanostructures, Nanomaterials

Lithiation Mechanisms of Si and Ge Thin Film Battery Electrodes

J. Miao, B. Wang, C. V. Thompson
Sponsorship: Skolkovo Institute of Science and Technology, SMART

Thin film batteries (TFBs) made using complementary metal-oxide-semiconductor- (CMOS) compatible materials and processes can be integrated with CMOS circuits and energy harvesting and sensing devices to produce low-cost autonomous sensors with small form factors. As part of our research on CMOS-compatible Li-ion TFBs, we are studying Si and Ge films to be used as anode electrodes. While these materials have the highest known charge capacity (8300 mA/cm³ for Si and 7300 mA/cm³ for Ge), they tend to have poor reliability (low cyclability) due to mechanical failures associated with large volume changes. The mechanisms through which lithium is stored in these materials are also poorly understood but are known to be related to poor cyclability. We have carried out mechanistic studies of reversible lithium storage in Si and Ge films using both electrochemical and physical characterization techniques.

Figure 1 shows current-voltage measurements made during the first three lithiation/delithiation cycles of a 315-nm-thick amorphous Si film (a cyclic voltammogram, CV). The current corresponds to Li being stored in the electrode (lithiation) or removed (delithiation). Peaks in these curves indicate accelerated charging or discharging associated with phase transitions, all of which are between amorphous phases with different stoichiometries (increasingly Li-rich for lithiation). An irreversible transition is seen in the first cycle (peak 1 in Figure 1), and two reversible transitions are seen in all three and all subsequent cycles (peaks 2-2' and 3-3'). Through new potentiostatic and transmission electron microscopy techniques, we have established that the irreversible transition occurs through propagation of a reaction through the thickness of the film (Figure 2b) and that the reversible transitions occur through an amorphous-to-amorphous nucleation and growth process (Figure 2b), sometimes referred to as a polyamorphous phase transition. In similar experiments on Ge, we have focused on the reversible transition of a Li-rich amorphous phase to a crystalline phase, which also occurs through a nucleation and growth process. These studies have been correlated with the reliability of TFBs.

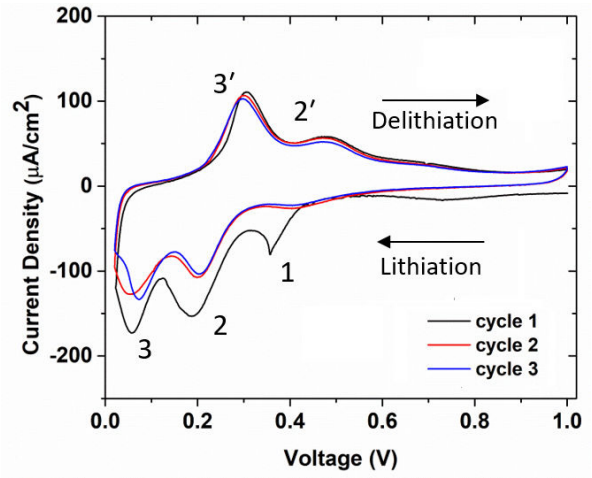

▲ Figure 1: CV for the first three cycles of a 315- nm-thick amorphous Si thin film. The current density is related to insertion of Li into Si during lithiation and removal of Li during delithia-tion. Peaks correspond to phase transitions.

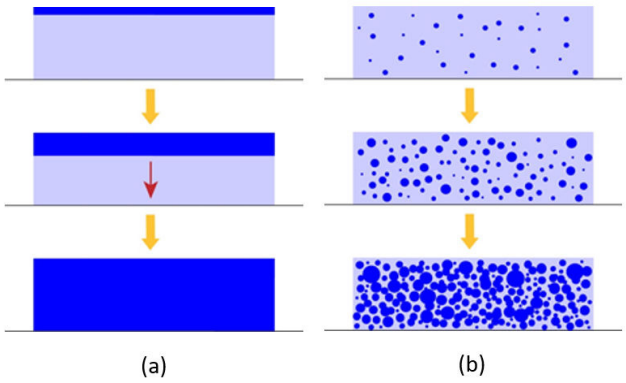

▲ Figure 2: Schematic illustrations of cross sections of Si films during phase transitions associated with peaks in Figure 1. (a) Irreversible propagation of a sharp interface between two amorphous phases (peak 1). (b) Reversible nucleation and growth transitions between two amorphous phases (peaks 2-2' and 3-3').

FURTHER READING

- J. Miao and C. V. Thompson, "Kinetic Study of the Initial Lithiation of Amorphous Silicon Thin Film Anodes," *J. Electrochem. Soc.*, vol. 165, pp. A650-A656, 2018.
- J. Miao, B. Wang, and C. V. Thompson, "First-order Amorphous-to-Amorphous Phase Transitions During Lithiation of Silicon Thin Films," *Phys. Rev. Materials*, vol. 4, p. 043608, 2020.
- J. Miao, B. Wang, and C. V. Thompson, "Kinetic Study of Lithiation-induced Phase Transitions in Amorphous Germanium Thin Films," *J. Electrochem.* Soc., vol. 167, p. 090557, 2020.

Gated Nonreciprocal Magnon Transmission from Direction-Dependent Magnetic Damping

J. Han, Y. Fan, B. C. McGoldrick, J. Finley, J. T. Hou, P. Zhang, L. Liu
Sponsorship: NSF, SRC

An important application of magnetic materials in information technology is to provide nonreciprocity, which allows unidirectional signal transmission. A representative device is the two-terminal microwave isolator. A ferromagnet inside naturally breaks the time-reversal symmetry and allows microwave transmission only from port 1 to port 2, while signals from port 2 to port 1 are suppressed. Despite wide applications, these conventional nonreciprocal devices suffer from their bulk volume and the difficulty of being integrated into high-density circuits. Nowadays, new mechanisms that can provide passive and directional isolation of signals are being pursued at sub-micrometer scale. Among various proposals, magnons, the quanta of the collective excitation of magnetic moments, show unique potential due to the tunability and the possibility for on-chip integration. So far, nonreciprocal magnon transmission has been achieved only at resonant conditions with gigahertz frequency. It is unclear if nonreciprocity can still be observed for magnons with a broad spectrum up to terahertz frequency.

Here we show that using a magnetic gate, one can realize tunable nonreciprocal propagation in spin Hall effect-excited incoherent magnons, whose frequency covers the spectrum from a few gigahertz up to terahertz. We further identify the direction-dependent magnetic damping as the dominant mechanism for the nonreciprocity, which originates from the interlayer dipolar coupling and works both in the ballistic and diffusive regions of magnons. As a natural result of the chiral magnon-magnon coupling, our findings provide a general mechanism for introducing directional magnon transmission and lead to a design of passively gated magnon transistors for applications of information transmission and processing.

Gigahertz Frequency Antiferromagnetic Resonance and Strong Magnon-Magnon Coupling in Layered Crystal $CrCl_3$

J. T. Hou, D. MacNeill, D. R. Klein, P. Zhang, P. Jarillo-Herrero, L. Liu
Sponsorship: DoE Office of Science, Gordon and Betty Moore Foundation, NSF, NSF GRFP

Magnon-magnon hybrid systems have recently been realized between two adjacent magnetic layers, with potential applications to hybrid quantum systems and coherent information processing. Realizing magnon-magnon coupling within a single material requires antiferromagnetic (AFM) or ferrimagnetic materials with magnetic sublattice structures. However, conventional AFM resonance lies in terahertz frequencies, which require specialized techniques to probe.

In this work, we realize strong magnon-magnon coupling within a single material, $CrCl_3$. $CrCl_3$ is a layered van der Waals AFM material, with parallel intralayer alignment and antiparallel interlayer alignment of magnetic moments (Figure 1). Because of weak anisotropy and interlayer magnetic coupling, we observe both optical and acoustic modes of AFM resonances within the range of typical microwave electronics (<20GHz), in contrast to conventional AFM resonances. By breaking rotational symmetry, we further show that strong magnon-magnon coupling with large tunable gaps can be realized between the two resonant modes (Figure 2). Our results demonstrate strong magnon-magnon coupling within a single material and establish $CrCl_3$ as a convenient platform for studying AFM dynamics in microwave frequencies. Because $CrCl_3$ is a van del Waals material that can be cleaved to produce air-stable monolayer thin films, these results open up the possibility to realize magnon-magnon coupling in magnetic van der Waals heterostructures by symmetry engineering.

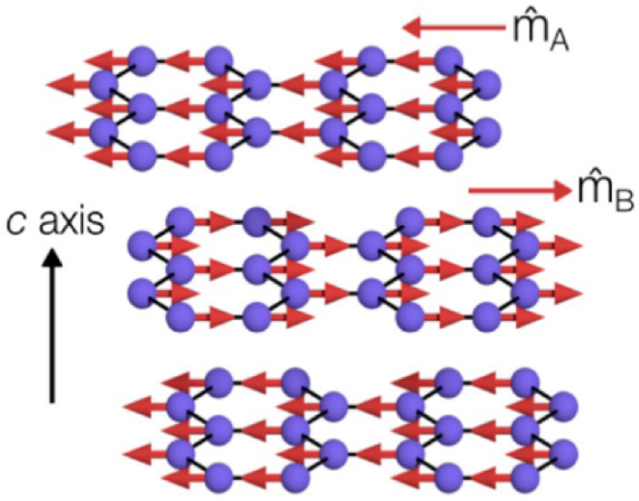

▲ Figure 1: Magnetic structure of bulk $CrCl_3$ below the Neel temperature. Blue spheres represent Cr atoms.

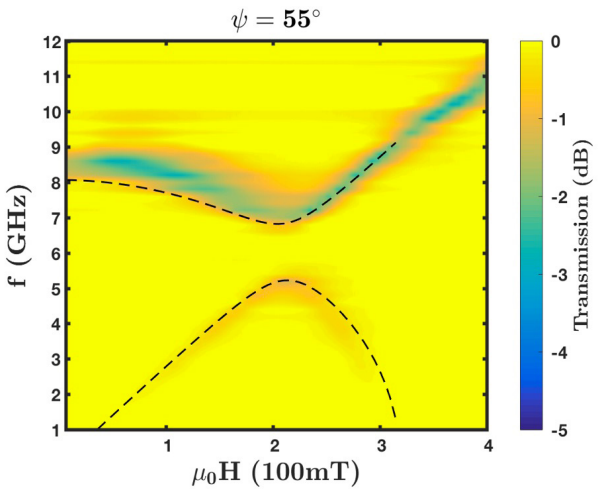

▲ Figure 2: Strong magnon-magnon coupling realized with magnetic field applied at a 55° angle with respect to the crystal plane.

FURTHER READING

- D. MacNeill, J. T. Hou, D. R. Klein, P. Zhang, P. Jarillo-Herrero, and L. Liu, *Physical Review Letters*, vol. 123, p. 047204, 2019.

Nanoparticle-Enhanced Microsputtered Gold Thin Films for Low-Cost, Agile Manufacturing of Interconnects

Y. Kornbluth, R. Mathews, L. Paramswaran, L. Racz, L.F. Velásquez-García
Sponsorship: US Air Force

Silicon and gold are ubiquitous in the microelectronics industry—silicon as the cornerstone of semiconductor devices, and gold as a material with unmatched electro-optical properties. However, gold films do not adhere well to silicon or silicon dioxide, necessitating the need for an adhesion layer made of a third material. This need increases complexity and cost. Also, reworking interconnects via traditional (cleanroom) technology poses challenges, e.g., thermal budget, vacuum compatibility.

In this project, we explore microplasma sputtering to implement at low-cost interconnects for agile electronics. We have shown that under proper operational conditions, a microplasma sputterer creates at room temperature and atmospheric pressure dense, highly conductive gold films with a fivefold better adhesion than the state of the art, without using an adhesion layer, annealing, or any other pre/post printing steps. If the gold film is sputtered in an atmospheric-pressure microsputterer in the presence of a fast-moving jet of air, gold nanoparticles form. The high collisionality of the atmospheric-pressure gas and high energy of the plasma facilitate nanoparticle formation, while the jet carries the nanoparticles to the substrate. The speed of the jet of air determines the size of the nanoparticles. These nanoparticles then act as an adhesion layer to allow a gold film, made of these nanoparticles and individual atoms, to adhere well to a silicon or silicon dioxide substrate. By rastering the printhead over the desired deposition area, we can interweave large nanoparticles and smaller atoms, creating a dense film (Figure 1). This process allows us to optimize adhesion, density, and conductivity simultaneously. Conductivity of the resultant films is also near-bulk (120% of bulk gold—the highest value reported for a room-temperature additive manufacturing method), allowing for their use in microelectronics.

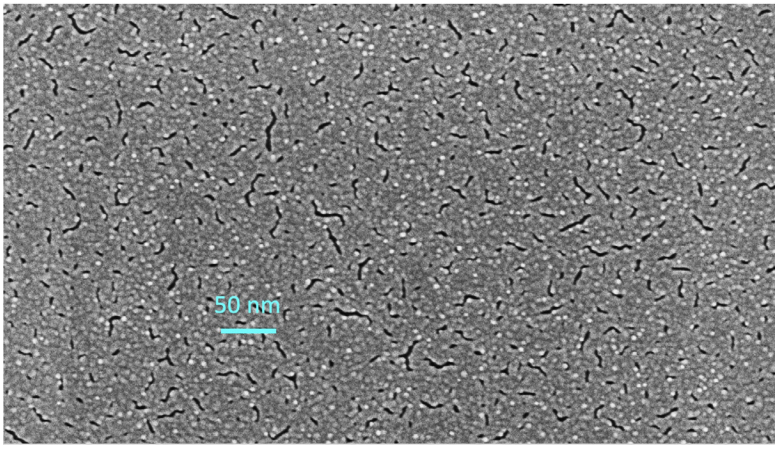

▲ Figure 1: SEM micrograph of microsputtered gold imprint (from Kornbluth et al., Additive Manufacturing, vol. 36, p. 101679, Dec. 2020). The film is dense, highly electrically conductive and is made of the agglomeration of nanoparticles created in the plume of a room-temperature, atmospheric pressure microsputterer.

FURTHER READING

- Y. Kornbluth, R. H. Mathews, L. Parameswaran, L. M. Racz, and L. F. Velásquez-García, "Nano-additively Manufactured Gold Thin Films with High Adhesion and Near-bulk Electrical Resistivity via Jet-assisted Nanoparticle-dominated, Room-temperature Microsputtering," *Additive Manufacturing*, vol. 36, p. 101679, Dec. 2020.
- Y. Kornbluth, R. H. Mathews, L. Parameswaran, L. M. Racz, and L. F. Velásquez-García, "Room-temperature, Atmospheric-pressure Microsputtering of Dense, Electrically Conductive, Sub-100 nm Gold Films," *Nanotechnology*, vol. 30, no. 28, p. 285602, Apr. 2019.
- Y. Kornbluth, R. H. Mathews, L. Parameswaran, L. M. Racz, and L. F. Velásquez-García, "Microsputterer with Integrated Ion-drag Focusing for Additive Manufacturing of Thin, Narrow Conductive Lines," *Journal of Physics D – Applied Physics*, vol. 51, no. 16, p. 165603, Apr. 2018.

Large-Scale 2D Perovskite/Transition Metal Dichalcogenide Heterostructure for Photodetector

D. Lee, S. Bae, J. Kim
Sponsorship: SUSTECH

Monolayer transition metal dichalcogenides (TMDCs) have been attractive nanomaterials for optoelectronics due to their extremely high quantum efficiency, but their atomically thin thickness prevents them from absorbing sufficient light for optoelectrical applications.

To improve the optoelectrical performance of TMDCs, during the past years, 2D Ruddlesden-Popper perovskites (PVSKs)/TMDC heterostructures have been demonstrated. Thanks to their high absorption coefficient, long diffusion length of charge carrier, sharp exciton emission, and high power conversion efficiency, 2D PVSKs have been used as an absorption layer for TMDCs. However, 2D PVSK/TMDC heterostructures are limited in the micrometer scale, since 2D PVSKs have been fabricated only by the tape-exfoliation method.

We reported a layer resolved splitting (LRS) technique to isolate multilayer 2D materials into a monolayer in wafer scale in 2018. To improve the scalability of 2D PVSKs for large-scale application, in this work, we successfully split micrometer-thick 2D PVSKs into nanometer-thick and millimeter-width scale with the LRS technique. We also obtained 90% of photoluminescence quantum yield, which is the world's best record to the best our knowledge. Then we plan to demonstrate large-scale 2D PVSK/TMDC heterostructures for photodetectors, which only has been previously demonstrated up to micrometer scale.

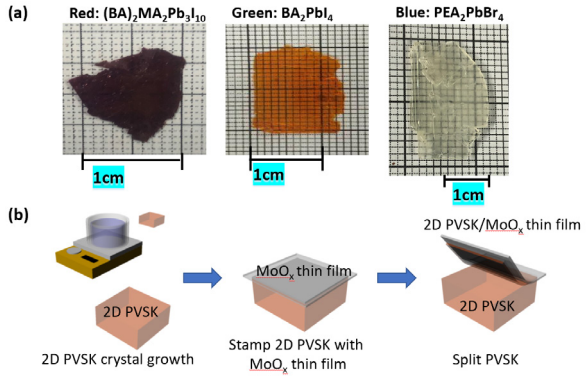

▲Figure 1: (a) Images of as-grown bulk 2D perovskite single crystals (b) schematic of stamping process to split 2D perovskite into atomic layer

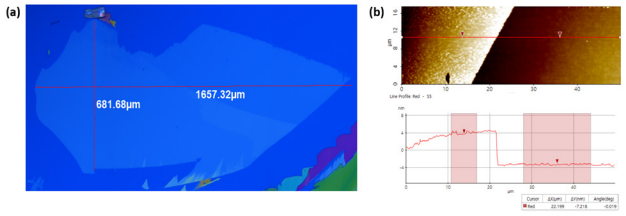

▲Figure 2: (a) Optical image of 8nm-thick and mm-width scale 2D perovskite layers (b) AFM image of split 2D perovskite layer.

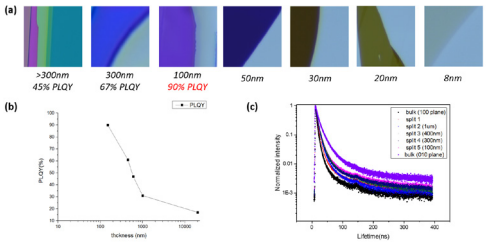

▲Figure 3: (a) Optical images of split 2D perovskite layers with different thinkness (b) Photoluminescence quantum yield (PLQY) of 2D perovskite with different thickness (c) Carrier lifetime of 2D perovskite with different thickness.

FURTHER READING

- J. Shim, et al., "Controlled Crack Propagation for Atomic Precision Handling of Wafer-scale Two-dimensional Materials," *Science*, vol. 362.6415 pp. 665-670, 2018.
- U. Erkılıç, et al., "Vapor Phase Selective Growth of Two-dimensional Perovskite/WS2 Heterostructures for Optoelectronic Applications." *ACS Applied Materials & Interfaces*, vol. 11, no. 43, pp. 40503-40511, 2019.
- Q. Wang, et al., "Optoelectronic Properties of a van der Waals WS2 Monolayer/2D Perovskite Vertical Heterostructure," *ACS Applied Materials & Interfaces*, vol. 12, no. 40, pp. 45235-45242, 2020.

Grayscale Stencil Lithography

X. H. Li, Z. J. Tan, N. Fang
Sponsorship: ExxonMobil

In this work, we demonstrate a new eBeam evaporation method with fixed single stencil shadow mask to generate 2D patterns with spatial thickness variation across wafer-scale substrate. This method outperforms conventional approaches like the iterative photo-lithography-and-lift-off method or grayscale photolithography, due to their limitations of efficiency, material choices, and manufacturing complexity. We applied the method to create a multi-spectral reflective color filter arrays with two layers of variable thickness. It offers a broader design space to achieve a wide color spectrum with simple and efficient fabrication procedures. This method shows potential for scaling up and high-resolution patterning, which could be widely applied in manufacturing for optical imaging, sensing, and computing.

The method takes inspiration from the "pin-hole imaging" in optics to generate the convoluted pattern of the material source and the stencil shadow mask, as shown in Figure 1.

The ejection of materials in the eBeam pockets is analogous to the "light source," which passes thorough the pin holes on the shadow masks to finally cast the "image" in terms of deposition thickness. By controlling the deposition dose (T) and the tilting angle (ϑ) of the substrate, we could create the "point spreading function" (PSF) of the material target passing through the shadow mask, which can create smooth deposition with less than 5-nm surface roughness. As show in Figure 2, we applied this method to create a multi-spectral color filter array and a 2D pattern of the MIT "Dome" to demonstrate the capability of this method for customizable patterning. Higher resolution deposition is also possible by combining the available micro/nano stencil lithography techniques and our grayscale stencil lithography method.

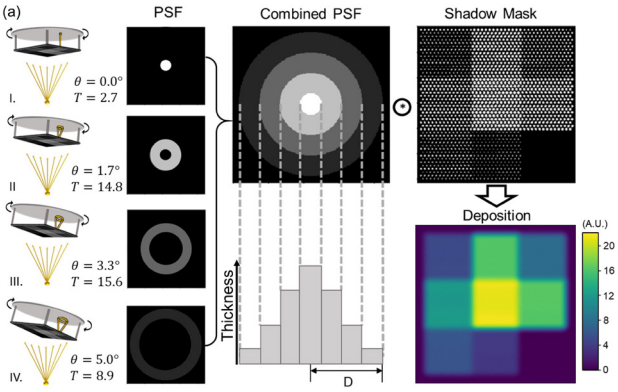

▲ Figure 1: Schematic of PSF control and convo-luted deposition of the grayscale stencil li-thography method.

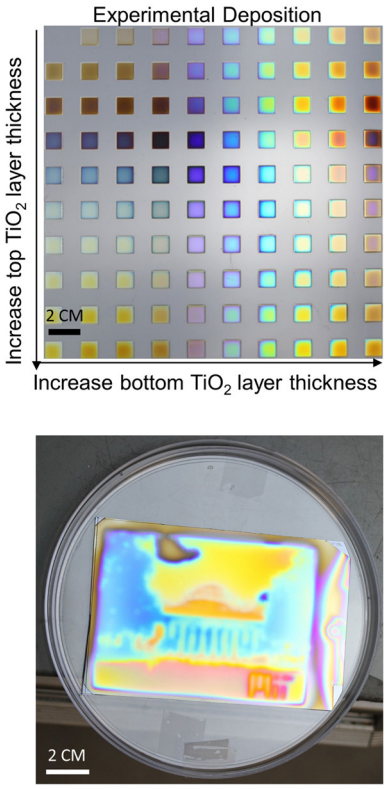

▶ Figure 2: Demonstration of spatially variable thickness deposition for multispectral color filter array and MIT "Dome."

FURTHER READING

- X. H. Li, Z. J. Tan, and N. Fang, "Grayscale Stencil Lithography for Patterning Multispectral Color Filters," *Optica*, vol. 7, no. 9, pp. 1154-1161, Sep. 2020.
- K. Du, J. Ding, Y. Liu, I. Wathuthanthri, and C.H. Choi, "Stencil Lithography for Scalable Micro and Nano Manufacturing," *Micromachines*, vol 8, no. 4, pp. 131–155, Apr. 2017.

Unraveling the Correlation between Raman and Photoluminescence in Monolayer Molybdenum Disulfide through Machine Learning Models

A.-Y. Lu, L. G. Pimenta-Martins, P.-C. Shen, J.-H. Park, Z. Chen, J. Han, J. Kong
Sponsorship: ISN

Two-dimensional (2D) transition metal dichalcogenides (TMDs) with intense and tunable photoluminescence (PL) have opened up new opportunities for optoelectronic and photonic applications such as light-emitting diodes, photodetectors, and single-photon emitters. Among the standard characterization tools for 2D materials, Raman spectroscopy stands out as a fast and non-destructive technique capable of probing materials' crystallinity and perturbations such as doping and strain. However, the correlation between photoluminescence and Raman spectra in monolayer MoS_2 remains elusive due to its highly nonlinear correlation. Here, we systematically explore the correlation between PL signatures and Raman modes through machine learning models. First, we adopt a convolution neural network, DenseNet, to predict PL by spatial Raman maps with relatively small pixel dimensions but deep channels. Moreover, we apply a gradient boosted trees model (XGBoost) with the Shapley additive explanation (SHAP) to evaluate the impact of individual Raman features in PL behavior, which allows us to further link the strain and doping of monolayer MoS_2 with its PL behavior. Our analytical method unravels the nonlinear correlations of physical or chemical properties for 2D materials and provides the knowledge for tuning and synthesizing 2D semiconductors for high-yield photoluminescence.

FURTHER READING

- Y. Kornbluth, R. H. Mathews, L. Parameswaran, L. M. Racz, and L. F. Velásquez-García, "Room-temperature, Atmospheric-pressure Microsputtering of Dense, Electrically Conductive, Sub-100 nm Gold Films," *Nanotechnology,* vol. 30, no. 28, p. 285602, Apr. 2019.
- Y. Kornbluth, R. H. Mathews, L. Parameswaran, L. M. Racz, and L. F. Velásquez-García, "Microsputterer with Integrated Ion-drag Focusing for Additive Manufacturing of Thin, Narrow Conductive Lines," *Journal of Physics D – Applied Physics*, vol. 51, no. 16, p. 165603, Apr. 2018.

Additively Manufactured Electrospray Ion Thrusters for Cubesats

D. Melo-Máximo, L. F. Velásquez-García
Sponsorship: MIT Portugal, MIT-Tecnologico de Monterrey Nanotechnology Program

Putting satellites in orbit is very expensive: typical rocket launches cost up to hundreds of millions of US dollars, and typical per-kilogram of payload costs are up to tens of thousands of US dollars). Therefore, great interest exists to develop smaller, lighter, and cheaper space satellites with adequate performance. In particular, since the 1990s, research groups across the world have been developing and launching cubesats, i.e., 1-10 Kg, a few L in volume, miniaturized, mission-focused satellites. Multi-material additive manufacturing is of great interest for fabricating cubesats, as it can monolithically create complex, multi-functional objects composed of freeform components made of materials matched to performance.

Electrospray engines produce thrust by electrohydrodynamically ejecting charged particles from liquid propellant. Electrospray thrusters are an attractive choice for propelling cubesats because their physics favors miniaturization, e.g., their start-up voltage scales with the square root of the emitter diameter. The thrust of an electrospray emitter is very low; thus , electrospray engines have large arrays of emitters to greatly boost the thrust they can deliver.

We recently demonstrated the first additively manufactured electrospray engines. Our devices are composed of large arrays of conical emitters coated by a conformal forest of zinc oxide nanowires (ZnONWs) that transport the propellant to the emitter tips (Figure 1). The ZnONWs provide a large hydraulic impedance that regulates and uniformizes the flow across the emitter array, restricting the flow rate per emitter to attain ionic emission. Our devices are also remarkable because, unlikely all the other electrospray ionic liquid engines reported in the literature, they emit only ions using the ionic liquid EMI-BF_4 as propellant (Figure 2), which maximizes their specific impulse for a given bias voltage, i.e., they produce more thrust per unit of propellant flow rate. Current work focuses on optimizing device design and fabrication and on developing a multi-electrode stack to control the plume.

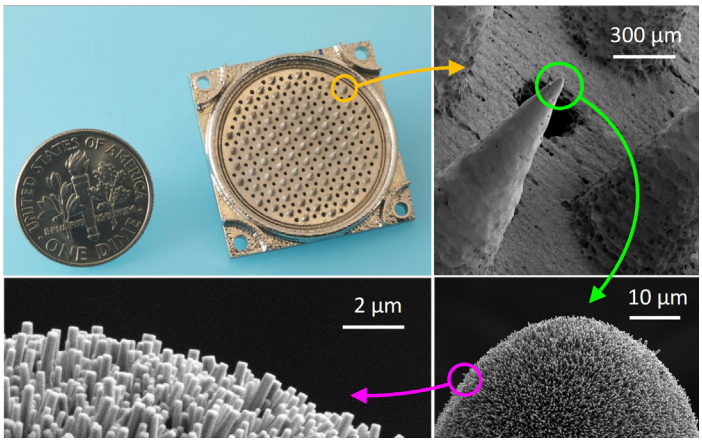

▲ Figure 1: From the top left, clockwise: an additively manufactured electrospray array next to a U.S. dime, close-up of emitters, close-up of an emitter tip, close-up of the ZnONW forest.

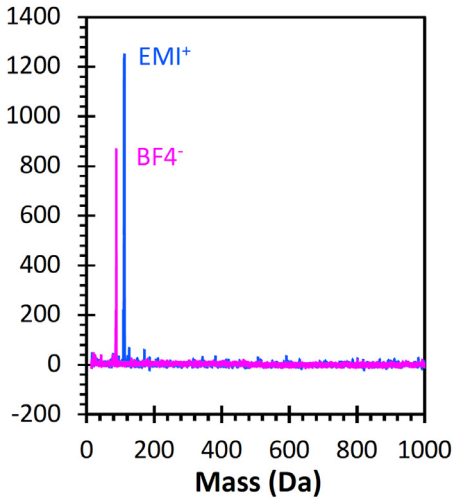

▲ Figure 2: Mass spectra of emitted plume using EMI-BF4 as propellant. In both polarities, the plume is composed exclusively of ions.

FURTHER READING

- F. A. Hill, E. V. Heubel, P. P. de Leon, and L. F. Velásquez-García, "High-Throughput Ionic Liquid Ion Sources Using Arrays of Microfabricated Electrospray Emitters with Integrated Extractor Grid and Carbon Nanotube Flow Control Structures," *J. Microelectromech. Syst.*, vol. 23, no. 5, pp. 1237-1248, May 2014.
- D. Olvera-Trejo and L. F. Velásquez-García, "Additively Manufactured MEMS Multiplexed Coaxial Electrospray Sources for High-Throughput, Uniform Generation of Core-Shell Microparticles," *Lab Chip*, vol. 16, no. 21, pp. 4121-4132, Oct. 2016.
- D. V. Melo Maximo and L. F. Velásquez-García, "Additively Manufactured Electrohydrodyna- mic Ionic Liquid Pure-Ion Sources for Nanosatellite Propulsion," *Additive Manufacturing*, vol. 36, p. 101719, Dec. 2020.

Low-Temperature Growth of High Quality MoS_2 by Metal-Organic Chemical Vapor Deposition

J.-H. Park, A.-Y. Lu, P.-C. Shen, J. Kong
Sponsorship: ARO MURI, NSF

The large-area and high-quality synthesis of molybdenum disulfide (MoS_2) plays an important role in realizing industrial applications of flexible, wearable, and ultimately scaled devices due to its atomically thin thickness, sizable bandgap, and dangling-bond-free interface. However, currently used synthesis of MoS_2 by chemical vapor deposition (CVD) require high temperature and a transfer process, which limits its utilization in device fabrications. In this work, we achieved the direct synthesis of high-quality monolayer MoS_2 by metal-organic chemical vapor deposition (MOCVD) at a low temperature of 320°C by designing the experimental setup for better controlling the flow rate of the organic precursors. Large single-crystal monolayer MoS_2 with a domain size up to 120 μm can be obtained on SiO_2/Si substrate (Figure 1). Owing to the low substrate temperature, the MOCVD-grown MoS_2 exhibits low impurity doping and nearly unstrained properties on the growth substrate, demonstrating enhanced electronic performance with high electron mobility of 68.3 $cm^2 V^{-1}s^{-1}$ at room temperature. In addition, we propose a model to quantitatively analyze the shape change of the MoS_2 flakes grown under different conditions, which provides an insight into the growth mechanism for optimizing growth conditions.

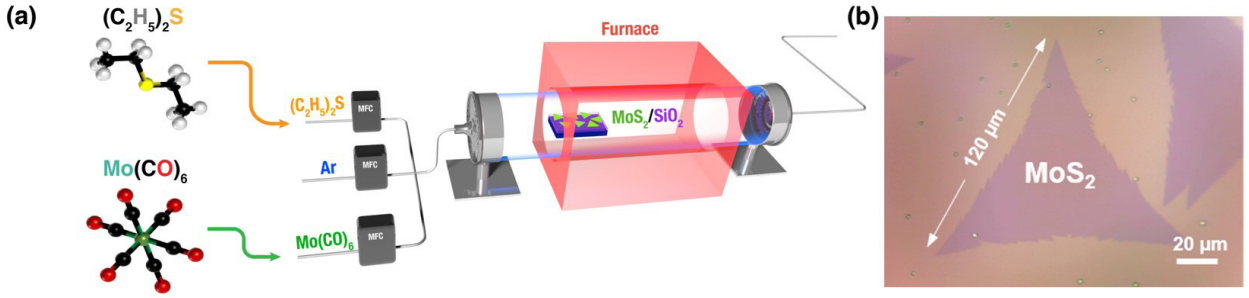

▲ Figure 1: (a) Schematic diagram of the experimental setup of the MOCVD system for MoS_2 growth and (b) Optical image of MoS_2 flake grown on SiO_2/Si substrate at low temperature.

FURTHER READING

- J.-H. Park, A.-Y. Lu, P.-C. Shen, B. G. Shin, H. Wang, N. Mao, R. Xu, S. J. Jung, D. Ham, K. Kern, Y. Han, and J. Kong, "Synthesis of High-Performance Monolayer Molybdenum Disulfide at Low Temperature," *Small Methods*, submitted.
- K. Kang, S. Xie, L. Huang, Y. Han, P. Y. Huang, K. F. Mak, C.-J. Kim, D. Mullller, and J. Park, "High-Mobility Three-Atom-Thick Semiconducting Films with Wafer-Scale Homogeneity," *Nature*, vol. 520, pp. 656-660, Apr. 2015.

Self-Assembly via Defect-Mediated Metal Nanoisland Nucleation on 2D Materials

K. Reidy, V. Zarubin, Y. Yu, I. Charaev, J. D. Thomsen, F. M. Ross
Sponsors: MIT OGE, Mathworks Engineering, Microscopy Society of America (MSA)

Patterning point defects, nanopores, and nanoribbons can enhance (opto-)electronic properties of two-dimensional (2D) materials. Moreover, metal adatoms and small clusters can nucleate on point defects in 2D materials. This nucleation suggests that defect patterning may be used for templated self-assembly of metal nanoislands on 2D materials, enabling applications in plasmonics and single-photon emission. Focused ion beams (FIBs) are well-suited for patterning 2D materials with nanometer precision and can be used for the controlled creation of point defects and sub-10-nm features. For applications that require control of the locations of metal islands, the optimization of FIB irradiation parameters for metal nucleation is crucial.

In this work, we study the structural changes that arise from FIB patterning of suspended 2D materials and the influence of patterning on metal nucleation and growth. We calibrate the irradiation parameters to achieve patterning with minimal damage to the 2D material, and the features are characterized by scanning transmission electron microscopy (STEM) (Figure 1a). Using these patterned 2D materials, we study the extent to which the defects, ion species, dose rate, and sample thickness affect the nucleation and growth of metals. Figure 1 shows representative results after the deposition of Au. At high deposition amounts, Au forms small islands around graphene nanopores, indicative of defect-mediated nucleation (Figure 1b). The templating and nucleation control presented here can be generalized to anchor other materials on 2D materials, such as Si and Ge via chemical vapor deposition or other metals via thermal and e-beam evaporation. This strategy opens routes towards the directed self-assembly of semiconducting and metallic nanoislands on 2D materials with optimized charge transfer and strong light-matter interactions.

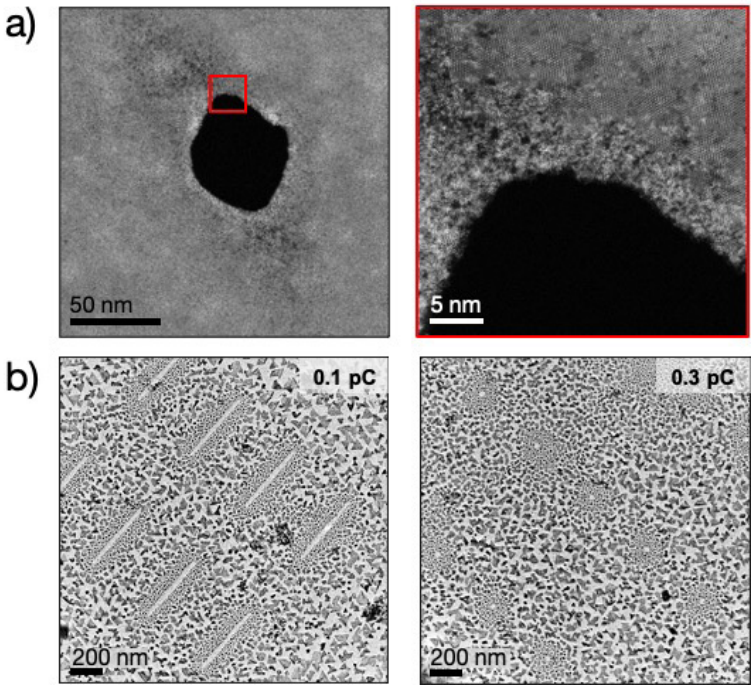

◀ Figure 1: STEM characterization of defects and deposition on defective 2D materials. a) Defect in monolayer MoS2 irradiated with He+ in the Helium Ion Microscope showing 50-nm hole created by ~600,000 He+ ions per spot irradiation. Right panel is a high magnification view of the amorphized region around a hole. b) Nucleation of Au islands on irradiated graphene flakes patterned with lines (left) and points (right), where Au appears as dark areas. Inset shows dose used.

FURTHER READING

- K. Reidy, G. Varnavides, J. D. Thomsen, A. Kumar, T. Pham, A.M. Blackburn, P. Anikeeva, P. Narang, J.M. LeBeau, F.M. Ross, "Direct Imaging and Electronic Structure Modulation of Moiré Superlattices at the 2D/3D Interface," *Nat. Comm.* vol. 12, pp. 1290, 2021, DOI:https://doi.org/10.1038/s41467-021-21363-5.
- J. Thomsen, K. Reidy, T. Pham, and F. M. Ross, "Nucleation and Growth of Metal Films and Nanocrystals on Two-dimensional Materials," *Microscopy and Microanalysis*, vol. 26, no. S2, pp. 1094-1096, 2020, DOI:10.1017/S1431927620016931.

Strain Control of Nanocatalyst Synthesis

J. Wang, B. Yildiz
Sponsorship: Exelon Corporation

A central theme in renewable energy technologies today is designing nanostructured catalysts for desired reactions. Exsolution generates stable and catalytically active metal nanoparticles via phase precipitation out of a host oxide. Unlike traditional nanoparticle infiltration techniques, the nanoparticle catalysts from exsolution are anchored in the parent oxide. This strong metal-oxide interaction makes the exsolved nanoparticles more resistant against particle agglomeration than the infiltrated ones. While exsolution is an exciting and promising pathway for generating stable oxide supported nanoparticles, rational control over the exsolved particles has yet to be achieved. In particular, controlling the size and density of the exsolved nanoparticles remains a big challenge.

In this work, we propose point defect formation in the oxide lattice to be the fundamental knob to control exsolution and demonstrate this approach in epitaxial $La_{0.6}Sr_{0.4}FeO_3$ (LSF) thin films. By combining in-situ surface characterization and ab-initio defect modeling, we show oxygen vacancy and Schottky defects to be the primary points defects formed upon Fe0 exsolution. Lattice strain tunes the formation energy, and thus the abundance of these defects, and alters the amount and size of the resulting exsolution particles. As a result, the tensile strained LSF with a facile formation of these critical point defects results in a higher Fe0 metal concentration, a larger density of nanoparticles, and reduced particle size at its surfaces. These observations highlight the critical role of point defects in controlling the size and density of the exsolved nanoparticles on the perovskite surface. The strain-controlled synthesis of nanocatalysts can benefit a wide range of applications in clean energy conversion and fuels generation such as solid oxide cells (SOCs), chemical looping (CL), and ceramic membrane reactors (CMRs).

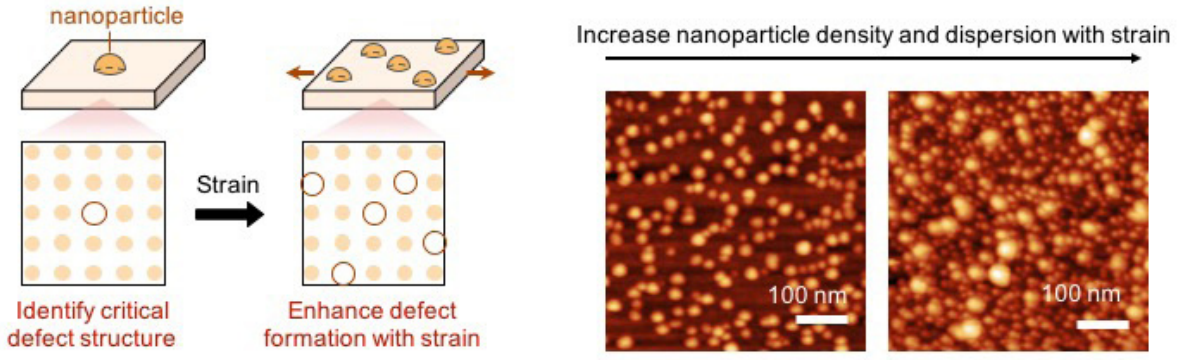

▲ Figure 1: Schematics and atomic force microscopy images showing lattice strain can facilitate nanoparticle synthesis by tailoring point defect formation in the host oxide.

FURTHER READING

- J. Wang, B. Yildiz et al., "Tuning Point Defects by Strain Modulates Nanoparticle Exsolution on Perovskite Oxides," under review.

Controlled Cracking to Improve Mechanical Stability of RuO_2 Thin-Film Li-ion Electrodes

L. Xu, C. V. Thompson
Sponsorship: SMART

Thin film Li-ion batteries are of interest for low-cost autonomous sensors. We have investigated high-performance electrode materials, such as Si and Ge for anodes and RuO_2 for cathodes, that can reversibly store high concentrations of Li. RuO_2 is of particular interest as a cathode material because of its ability to reversibly store high concentrations of Li without requiring high-temperature processing, unlike conventional cathode materials. While high Li capacities are beneficial for high energy density, high Li concentrations lead to large volume changes, which can lead to mechanical degradation during battery cycling. In particular, removal of Li (delithiation) leads to tensile stresses that can cause cracking and delamination of electrodes, which can severely limit the number of times that batteries can be charged and discharged.

Motivated by the finding that patterned small patches of Si demonstrated higher mechanical stability compared to continuous films, patterned arrays of holes with stress-raising corners were fabricated within sputtered RuO_2 thin films (Figures 1a and b). After lithiation and delithiation, channel cracks form along the directions defined by the hole array (Figure 1c). We found that this method for controlled crack formation led to increased mechanical stability, as no delamination occurred within the patterned area (Figure 2, right side), while severe delamination occurred in the unpatterned areas (Figure 2, left side). These results may occur because the formation of the controlled crack array dissipates the strain energy that would otherwise drive delamination.

It was further discovered that the formation of cracks was reversible. After re-lithiation, the RuO_2 patches expanded, and the channel cracks closed again (Figure 1d). The sizes of the channel cracks were controlled by the state of charge of the film. In addition to use for mechanical stabilization of thin film electrodes, this process has potential application for creation of channel networks with electrochemically modulated channel sizes, which might be of use in microfluidic devices.

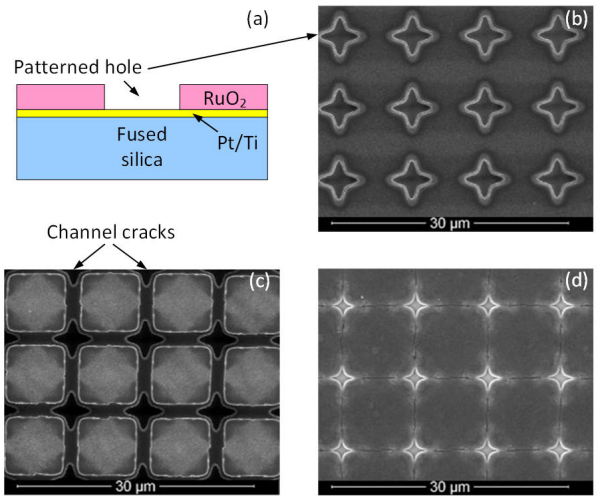

▲ Figure 1: (a) Schematic cross-section and (b) top-view SEM image of a patterned RuO2 film; (c) channel cracks formed after lithiation and delithiation and (d) channel cracks closed after re-lithiation.

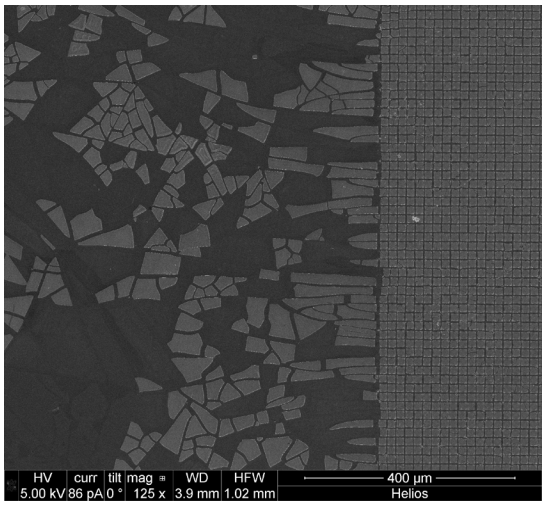

▲ Figure 2: Comparison of unpatterned RuO2 film (left side) and patterned film (right side) after cycling.

FURTHER READING

- D. Perego, J. S. T. Heng, X. Wang, Y. Shao-Horn, and C. V. Thompson, "High-performance Polycrystalline RuOx Cathodes for Thin Film Li-ion Batteries," *Electrochim. Acta*, vol. 283, pp. 228–233, 2018.
- L. Xu and C. V. Thompson, "Mechanisms of the Cyclic (de)lithiation of RuO2," *J. Mater. Chem.* A, vol. 8, pp. 21872–21881, 2020.

Seeing Superlattices: Imaging Moiré Periods at the Nanoisland-2D Material Interface Using Scanning Transmission Electron Microscopy

K. Reidy, G. Varnavides, J. Dahl Thomsen, A. Kumar, T. Pham, A. M. Blackburn, P. Anikeeva, P. Narang, J.M. LeBeau, F. M. Ross
Sponsorship: MIT MathWorks Engineering, MIT OGE, Office of Naval Research (ONR)

Opportunities are emerging to combine van der Waals (2D) materials with (3D) metals /semiconductors to explore fundamental charge-transport phenomena at their interfaces and exploit them for devices. Recent advances in scanning transmission electron microscopy (STEM) allow detailed analysis of atomic structure, properties, and ordering at these interfaces. We use 4D STEM and integrated differential phase contrast (iDPC) to directly image moiré periodicities arising from epitaxial growth of nanoislands on 2D materials in ultra-high vacuum. Our research explores the role of emerging microscopy techniques in unveiling the alignment and ordering of moiré superlattices and the implications of moiré periodicities for the properties of 2D/3D junctions.

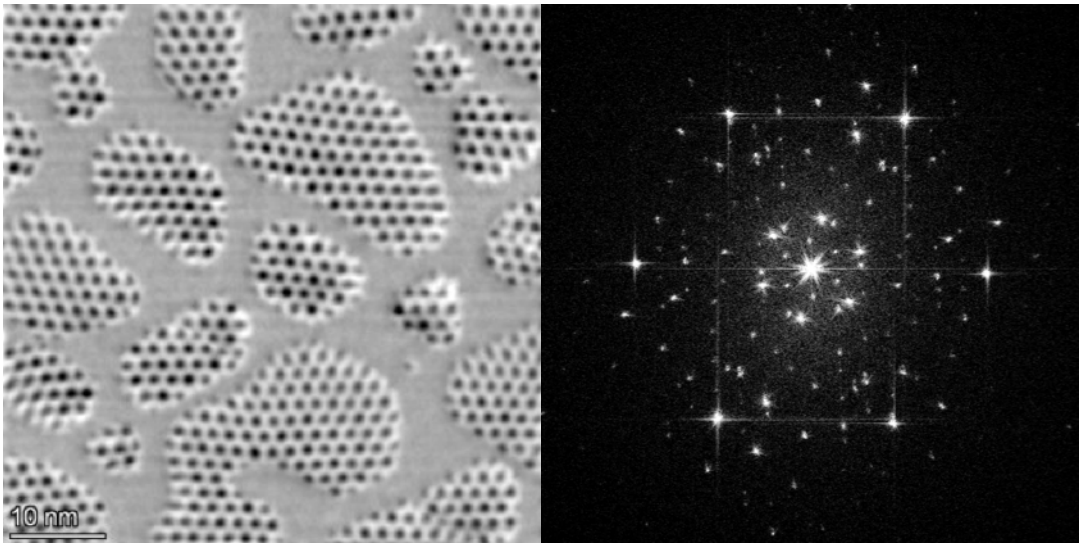

▲ Figure 1: Characterization of 2D/3D moiré superlattices: a) Integrated differential phase contrast (iDPC) STEM image of Au on MoS2 showcasing the moiré cells. b) Fast fourier transform (FFT) of atomic resolution high-resolution TEM image of the Au on MoS2 showing 1/3{422} reflection and visible moiré periodicities around the central spot. Illustrative yellow dots represent frequencies from Au crystal planes, while purple represent frequencies from MoS2 crystal planes. Scale bar, 0.5 Å−1

FURTHER READING

- K. Reidy, et al.,, "Direct Imaging and Electronic Structure Modulation of Moiré Superlattices at the 2D/3D Interface," *Nat. Comm.* vol. 12, pp. 1290, 2021, DOI:https://doi.org/10.1038/s41467-021-21363-5

Small-Molecule Assemblies Inspired by Kevlar: Aramid Amphiphile Nanoribbons

T. Christoff-Tempesta, Y. Cho, D.-Y. Kim, J.H. Ortony
Sponsorship: NSF, J-WAFS, Professor Amar G. Bose Research Grant Program

Small-molecule self-assembly offers a powerful bottom-up approach to producing nanostructures with high surface areas, tunable surfaces, and defined internal order. Historically, the dynamic nature of these systems has limited their use to specific cases, especially biomedical applications, in solvated environments. Here, we present a self-assembling small-molecule platform, the aramid amphiphile (AA), which overcomes these dynamic limitations. AAs incorporate a Kevlar-inspired domain within each molecule to produce strong interactions between molecules. We observe that AAs spontaneously form nanoribbons when added to water with aspect-ratios exceeding 4000:1. Robust internal interactions suppress the ability of AAs to move between assemblies and result in nanoribbons with mechanical properties rivaling silk. We harness this stability to extend small-molecule assemblies to the solid-state for the first time, forming macroscopic threads that are easily handled and support 200 times their weight when dried. The AA platform offers a novel route to use small-molecule self-assembly to achieve aligned nanoscale materials in the solid-state

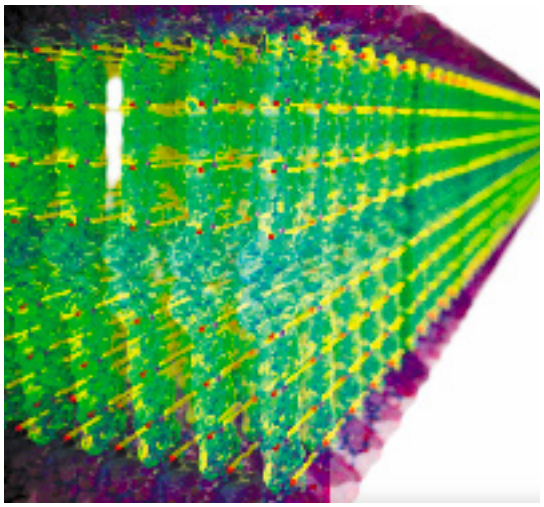

▲ Figure 1: Illustration of a nanoribbon constructed from the spontaneous self-assembly of aramid amphiphiles in water, with strong hydrogen bonding interactions between molecules shown in yellow.

FURTHER READING

- T. Christoff-Tempesta, Y. Cho, D.-Y. Kim, M. Geri, G. Lamour, A.J. Lew, X. Zuo, W.R. Lindemann, and J.H. Ortony, "Self-assembly of Aramid Amphiphiles into Ultra-stable Nanoribbons and Aligned Nanoribbon Threads," *Nature Nanotechnology*, vol. 16, pp. 447-454, January 2021
- T. Christoff-Tempesta, D.-Y. Kim, G. Lamour, X. Zuo, K.-H. Ryu, and J.H. Ortony, "Morphological Transitions of a Photoswitchable Aramid Amphiphile Nanostructure," *Nano Letters*, vol. 21, pp. 2912-2918, March 2021
- T. Christoff-Tempesta and J.H. Ortony, "Aramid Amphiphile Nanoribbons for the Remediation of Lead from Contaminated Water," *Environmental Science: Nano*, May 2021